Discrimination of Walking Patterns Using Wavelet-Based Fractal Analysis

Masaki Sekine, *Associate Member, IEEE*, Toshiyo Tamura, *Member, IEEE*, Metin Akay, *Senior Member, IEEE*, Toshiro Fujimoto, Tatsuo Togawa, *Senior Member, IEEE*, and Yasuhiro Fukui, *Member, IEEE*

Abstract—In this paper, we attempted to classify the acceleration signals for walking along a corridor and on stairs by using the wavelet-based fractal analysis method. In addition, the wavelet-based fractal analysis method was used to evaluate the gait of elderly subjects and patients with Parkinson's disease. The triaxial acceleration signals were measured close to the center of gravity of the body while the subject walked along a corridor and up and down stairs continuously. Signal measurements were recorded from 10 healthy young subjects and 11 elderly subjects. For comparison, two patients with Parkinson's disease participated in the level walking. The acceleration signal in each direction was decomposed to seven detailed signals at different wavelet scales by using the discrete wavelet transform. The variances of detailed signals at scales 7 to 1 were calculated. The fractal dimension of the acceleration signal was then estimated from the slope of the variance progression. The fractal dimensions were significantly different among the three types of walking for individual subjects ($p < 0.01$) and showed a high reproducibility. Our results suggest that the fractal dimensions are effective for classifying the walking types. Moreover, the fractal dimensions were significantly higher for the elderly subjects than for the young subjects ($p < 0.01$). For the patients with Parkinson's disease, the fractal dimensions tended to be higher than those of healthy subjects. These results suggest that the acceleration signals change into a more complex pattern with aging and with Parkinson's disease, and the fractal dimension can be used to evaluate the gait of elderly subjects and patients with Parkinson's disease.

Index Terms—Acceleration, fractal dimension, gait, walking, wavelet transform.

I. INTRODUCTION

MANY PREVIOUS studies have proposed to monitor and assess physical activities using an accelerometer. Accelerometry is a suitable method for measuring daily behavior without constraining the subject. The accelerometer output has a good relationship to energy consumption, which is widely accepted as the standard reference for physical activities [1]–[3]. Measuring physical activity in elderly people is useful not only as an aid in improving physical condition but also as a means of checking the amount of appropriate daily exercise. However, precise evaluation using accelerometry requires classification of the different types of activities since the relationship between energy consumption and accelerometer output for all physical activity may not be easily expressed.

Classification of daily activities, including standing, sitting, lying, and walking, has been done using a combination of dc and ac acceleration signals [4]–[6]. For a more precise evaluation, the data must be classified into different types of walking and to lead the relations between energy consumption and acceleration for each walking type since this relationship during walking on a corridor may not be the same for walking on stairs. Aminian *et al.* estimated the incline and the speed of walking by using two artificial neural networks [7]. The inputs consisted of 10 parameters that characterize the walking types between two heel-strikes.

Our previous study classified walking along a corridor and on stairs by using wavelet transform [8], [9]. These studies demonstrated that the method was effective for classifying walking types for young subjects but not for elderly subjects, since gait changes with age. In particular, locomotion is slower for elderly people than for young people. The amplitude of impact acceleration at heel-strike decreases with age. Elderly people also shuffle along the corridor, and complexity of acceleration increases. Therefore, it is difficult to classify the walking type by using the former proposed methods.

The acceleration signal can also be used for assessing the decline of physical function with aging. Furthermore, a patient who has a condition such as Parkinson's disease must be diagnosed at an early stage for normal daily activity to be maintained. With early diagnosis, it is easier to plan pharmacotherapy and rehabilitation. In the usual procedure for assessing physical function, a physiotherapist observes the gait of an elderly person or patient and evaluates the decline in physical function and the level of impairment. More precise kinetic and kinematic analyses are also carried out using optoelectronic systems and the force plate [10]–[13]. These systems are powerful but can assess only a few strides. They are also expensive and require a high level of technical skill and specialized experience to operate. In order to measure natural locomotion without restricting the subject to a walkway where the instruments were installed, instrumented shoes have been proposed [14], [15]. These instru-

mented shoes have some strain-gauge force transducers at the toe and heel. Although they provide outputs corresponding to the ground reaction force, they are not suitable as a portable device in daily life.

The capacitive sensors can measure the pressure between the foot and ground [16]–[18]. These sensors can be used for monitoring gait because they are lightweight and thin. However, their sensitivity changes when the load is not uniform but localized and the relationship between the load and changes of capacity is not linear. Most of the capacitive sensors also require long cables for connection to the portable measurement unit, which is often worn at the waist.

The accelerometry, on the other hand, has been proposed to measure the kinematics of body motion as well [19], [20]. The accelerometers are sufficiently small (on the order of a square centimeter) and lightweight (a few gram). They can be easily attached on the body and be included into the portable unit. Therefore, the accelerometry is advantageous to monitor the activity in daily life.

Wavelet analysis methods are finding a rapidly growing number of applications in fields ranging from physics to medicine. Specifically, it has become a powerful alternative for the analysis of nonstationary signals whose spectral characteristics are changing over time, since the widely used spectral analysis method provides only the frequency contents of the signals without providing the time localizations of the observed frequency components. This is very important in biological signal analysis since most of the statistical characteristics of these signals are nonstationary. Therefore, in practice, the wavelet transform method is appropriate for the analysis of biological signals consisting of short-lived, high-frequency components closely located in time as well as long duration components closely spaced in frequency [21].

The acceleration signal during walking represents both the complex pattern and the nonstationary property. The complexity of the signal can be quantified by the fractal dimension [22]. In this study, wavelet-based fractal analysis was chosen because the wavelet transform is an appropriate method for the analysis of both stationary and nonstationary biological signals [21].

The advantage of using the wavelet-based fractal analysis is indeed twofold. First, we analyze the nonstationary acceleration signal using the wavelet transform. Then, the time-frequency information contents obtained with the wavelet transform will be used to estimate the fractal value as detailed in the method section to characterize the acceleration signal during walking along the corridor and on the stairs. The estimation of the Hurst exponent (or the fractal dimension) is nothing more than a representation of the variances of the wavelet coefficients at each scale, which provides valuable information about the variance progression over the wavelet scales. In addition, it was applied to evaluate the acceleration signals in elderly subjects and subjects with Parkinson's disease.

II. MEASUREMENT SYSTEM

A schematic diagram of the experimental setup is shown in Fig. 1. This measurement system consisted of a triaxial
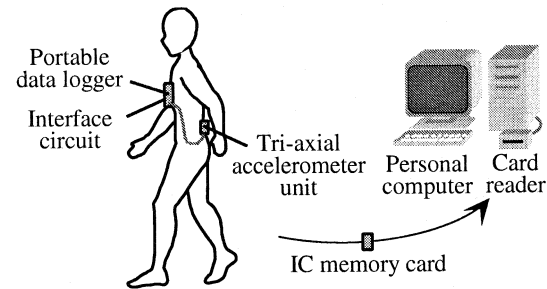

Fig. 1. Experimental setup.

accelerometer unit, an interface circuit, a portable data recorder, an IC memory card, a card reader, and a personal computer.

The accelerometer unit consisted of three uniaxial accelerometers (type 3031-010; IC-Sensors USA; size: $4 \times 4 \times 3$ mm; weight: 0.3 g; range: ± 10 g; frequency response: 0–500 Hz). These were mounted orthogonally to record signals in the anteroposterior (x), lateral (y), and vertical (z) directions. The accelerometers were calibrated by measuring their outputs under controlled inclination. For example, the outputs were 1 g, 0 g, -1 g, with the inclination at $0°$, $90°$, $180°$, respectively. After the accelerometer unit had been calibrated, it was fixed on an acrylic plate that had two slits for a waistbelt. Using an elastic waistbelt, the accelerometer unit was attached to the subject's back in the lumbosacral region of the vertebral column, close to the subject's center of gravity while standing.

The accelerometer unit was connected to a portable data logger[1] [4] via an interface circuit of our own fabrication. This data logger consisted of a CPU, 10-bit A/D converter, an IC card interface, and a removable 2-MB IC memory card. The interface circuit included three amplifiers and three second-order analog Butterworth low-pass filters as an anti-aliasing filter for each direction. Their cutoff frequencies were 500 Hz. The accelerometer outputs were digitized at a sampling rate of 1024 Hz by the data logger and were recorded on the IC memory card. After the measurements were completed, the data were transferred via a card reader to a PC for further analysis.

III. EXPERIMENTAL DESIGN

The experiments were performed with 10 healthy young subjects (age 22.6 ± 1.9 years, height 166.3 ± 5.9 cm, weight 58.7 ± 7.1 kg; mean $\pm$ SD) and 11 healthy elderly subjects (age 69.3 ± 5.6 years, height 154.0 ± 7.8 cm, weight 50.4 ± 9.6 kg; mean $\pm$ SD). For comparison, two patients with Parkinson's disease (age 60.5 years, height 156.5 cm, weight 50 kg; mean, Hoehn-Yahr stage II) participated in this study. None of the subjects used an orthosis or cane during walking.

The healthy subjects walked continuously over an indoor course at free speed (Fig. 2). The walking course started along a corridor, then continued downstairs, along another corridor and upstairs to return to the starting point. The length of each corridor was 20 m. The stairways consisted of 20 steps and included a landing between the steps 10 and 11. The slope of the stairways was $36.1°$. The healthy subjects did not use the handrails for support on the stairs. For the patients with
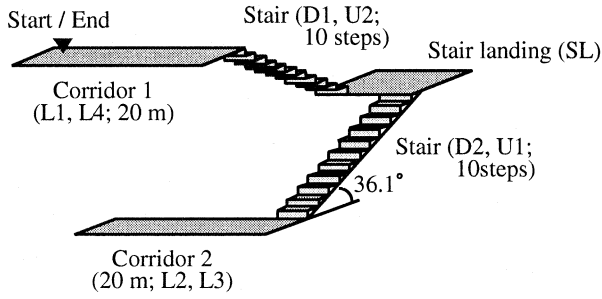
[1]Micro 8, Shimadzu, Kyoto, Japan.

Fig. 2. Experimental course. The subject began walking along corridor 1 (L1), walked down the stairs (D1, D2), walked along corridor 2 (L2 and L3, which were before and after the turn, respectively), climbed the stairs (U1, U2) and walked along corridor 1 again.

Parkinson's disease, measurement was performed only along the corridor. A video recording was made simultaneously to confirm walking types. To evaluate the reproducibility of the fractal dimension of acceleration, all subjects repeated the measurement within one week. This study was approved by the ethics committee of Fujimoto Hospital, and all the subjects gave written informed consent before examination.

IV. SIGNAL PROCESSING

A. Wavelet Transform

A discrete wavelet transform uses a set of basis functions to decompose a signal into the detailed signals d_{2^j} and the approximate signals a_{2^j} of the original signal. There are two basic functions in the design of a wavelet transform system. The first one is the scaling function ϕ, which is called the basic dilation function. The second one is the primary wavelet function ψ. The discrete wavelet transformation of a signal $x(n)$ is defined in the following equations [23]–[25]:

$$a_{2^J}(k) = \int x(n)\phi_{J,k}(n)dn \tag{1}$$

$$d_{2^j}(k) = \int x(n)\psi_{j,k}^*(n)dn \tag{2}$$

$$x(n) = \sum_{j=1}^{J}\sum_{k \in Z} d_{2^j}(k)\psi_{j,k}(n) + \sum_{k \in Z} a_{2^J}(k)\phi_{J,k}(n) \tag{3}$$

where j is the scale that represents the dilation index and k represents the index in time. J is the depth of the decomposition level and $*$ denotes complex conjugation. The wavelet and scaling functions are defined as

$$\phi_{j,k}(n) = 2^{-j/2}\phi\left(2^{-j}n - k\right) \tag{4}$$

$$\psi_{j,k}(n) = 2^{-j/2}\psi\left(2^{-j}n - k\right). \tag{5}$$

Here, j controls the dilation or compression of the scaling function $\phi_{j,k}(n)$ and the wavelet function $\psi_{j,k}(n)$. The scaling function and wavelet function have the essential properties of low-pass and bandpass Fourier transform, respectively.

The approximate signal $a_{2^0}(n)$ at scale $j = 0$ is equivalent to the original signal $x(n)$. The signal $a_{2^j}(n)$ at lower resolutions represents smoothed $a_{2^{j-1}}(k)$. The detailed signals $d_{2^j}(n)$ are given by the difference between approximate signals $a_{2^j}(n)$ and $a_{2^{j-1}}(k)$. The approximate signals $a_{2^j}(n)$ and the detailed signals $d_{2^j}(n)$ are replaced by the following equations:

$$a_{2^j}(n) = \sum_k h(k - 2n)a_{2^{j-1}}(k) \tag{6}$$

$$d_{2^j}(n) = \sum_k g(k - 2n)a_{2^{j-1}}(k) \tag{7}$$

where h and g represent the coefficients of the discrete low-pass and high-pass filters associated with the scaling function and the wavelet function, respectively.

B. Wavelet-Based Fractal Estimation

A fractal concept has been widely used to describe objects in space. In addition, it has been proposed to describe the characteristics of signals in time, including white noise and Brownian motion. The power spectrum density of these processes is generally defined by the following empirical equation [24], [26], [27]:

$$S(\omega) \sim \frac{\sigma^2}{|\omega|^\beta} \tag{8}$$

where ω is the frequency, σ^2 is the variance of the original signal, and β is the spectral component (the slope that gets the spectral density over several decades of frequency). In particular, the slope β is 0 for white noise and 2 for Brownian motion.

β has been proposed to be related to the parameter H, which shows its statistical self-similarity property as $H = (\beta - 1)/2$. For a one-dimensional signal, H is directly related to the fractal dimension D as $D = 2 - H$ in the range $1 < D < 2$ ($0 < H < 1$). As the values of D approach 1, the shape of the signal is smooth. Conversely, as the values of D approach 2, the shape of the signal is very complex.

Recently, the discrete wavelet transform method based on orthonormal wavelet decomposition was proposed to estimate the slope β, parameter H, and fractal dimension D [24], [25], [27].

Here, we briefly explain this approach. The frequency band of detailed signal d_{2^j} is represented as $fs/2^{j+1} < \omega < fs/2^j$ with sampling rate fs. Thus, the $S(\omega)$ in (8) can replace the variance of detailed signal d_{2^j}. The variance of d_{2^j} at each scale j can be given for the orthonormal wavelet decomposition as follows:

$$Variance\,(d_{2^j}) \sim \frac{\sigma^2}{(2^j)^\beta} \tag{9}$$

where slope β is calculated from the log-scale plot of the variance versus the resolution. The variance of the detailed signal at scale j is given as

$$Variance\,(d_{2^j}) = \left\{\frac{1}{(N_j - 1)}\right\}\sum\left(d_{2^j} - m_{d_{2^j}}\right)^2 \tag{10}$$

where $m_{d_{2^j}}$ is the mean of the detailed signal at scale j and N_j represents the number of samples of the detailed signal at scale j.

To detect changes in walking type, namely fractal dimension D over time course, slope β was calculated by a temporal window that contained 1024 samples (1 s) of raw data. After
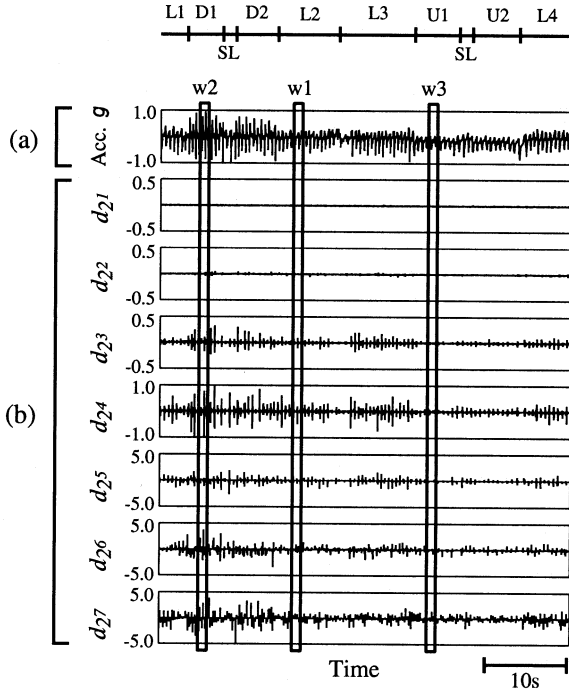
Fig. 3. Typical examples of the original acceleration signal in the x direction and detailed signals on scales 1 to 7 in healthy young subjects. The segments along the x axis are shown in Fig. 2. Windows (w1, w2, and w3) in Fig. 3 represent examples of the stationary acceleration during level walking, walking downstairs, and walking upstairs, respectively.
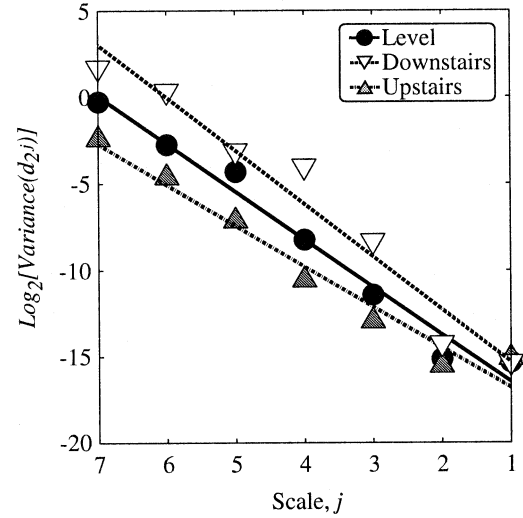

Fig. 4. Typical examples of log-scale plots of variances of d_{2j} versus scales at the temporal windows shown in Fig. 3. The circles, inverted triangles, and triangles indicate level walking, walking downstairs, and walking upstairs, respectively.

slope β had been determined, parameter H and fractal dimension D were estimated. This process was repeated in the next temporal window with an overlap of 512 samples (0.5 s). Therefore, the time resolution for estimation of the fractal dimension was 0.5 s. This resolution was considered to be sufficient for monitoring because the duration of one step is approximately 0.5 s [10].

In this paper, the acceleration signals were decomposed into seven levels using Daubechies wavelets with order $N = 4$ [23]. This order N determines the support length of wavelet function ψ and scaling function ϕ as $2N - 1$. The number of vanishing moments of wavelet function ψ is N. We used seven levels to estimate the fractal dimension since we were unable to estimate the slope using the very low frequency scales 8, 9 and 10. Note that the sampling frequency was chosen as 1024 Hz in order to have enough samples at low-frequency wavelet scales using the orthogonal wavelet transform and to have reliable variance estimates for calculating the fractal dimension.

V. RESULTS

Fig. 3(a) is an example of the recorded acceleration signal in the x direction when a healthy subject walked on the experimental course. Fig. 3(b) shows the detailed signal d_{2j} of the acceleration signal shown in Fig. 3(a). The length of sequence d_{2j} was halved when the data were decomposed by the discrete wavelet transform.

Fig. 4 shows the log-scale plots of the variance of the detailed signals at scales 7 to 1 in the temporal windows of the walking types shown in Fig. 3. Note that the walking type was

confirmed by the video recording. The slope of variance progression was different for the three types of walking. In this subject, slope β_X was 2.753 during walking along the corridor. Compared with level walking, walking downstairs had a steeper slope ($\beta_X = 2.882$) and walking upstairs had a less steep slope ($\beta_X = 2.339$). Accordingly, the fractal dimensions D_X were 1.124, 1.059, and 1.331 for walking along the corridor, walking downstairs, and walking upstairs, respectively.

Fig. 5 shows typical examples of the recorded acceleration signal in the x direction and its fractal dimension D_X through the experiment. When the subject walked downstairs or walked upstairs, D_X changed to a lower or higher value, respectively, compared with the D_X of level walking. In this case, by determining two optimal threshold levels, it was possible to find the time when each of the three types of walking began and ended. Before the experiment, the subject walked a predetermined course, and the observer knew the exact distance of each type of walk, such as level walking, walking upstairs, and walking downstairs. From these walking tests, we compared the walking type obtained from acceleration signals and fractal dimensions and determined the threshold levels.

Table I shows the averages of D_X, D_Y, and D_Z during each walking type for all healthy subjects. For most subjects, the fractal dimensions tended to shift to higher values during walking upstairs. In other words, the acceleration signals changed to a complex pattern when the subjects walked upstairs. On the other hand, for walking downstairs, there was no common feature in the fractal dimension among subjects. However, the fractal dimensions showed significant differences among walking types for individual subjects.

To determine significant differences, the fractal dimensions were statistically analyzed using the Kruskal–Wallis test and the Bonferroni multiple comparison method. In fractal dimension D_X, the differences between level and downstairs, level and upstairs, and downstairs and upstairs were statistically significant within 14 of 22, 22 of 22, and 21 of 22 subjects, respectively
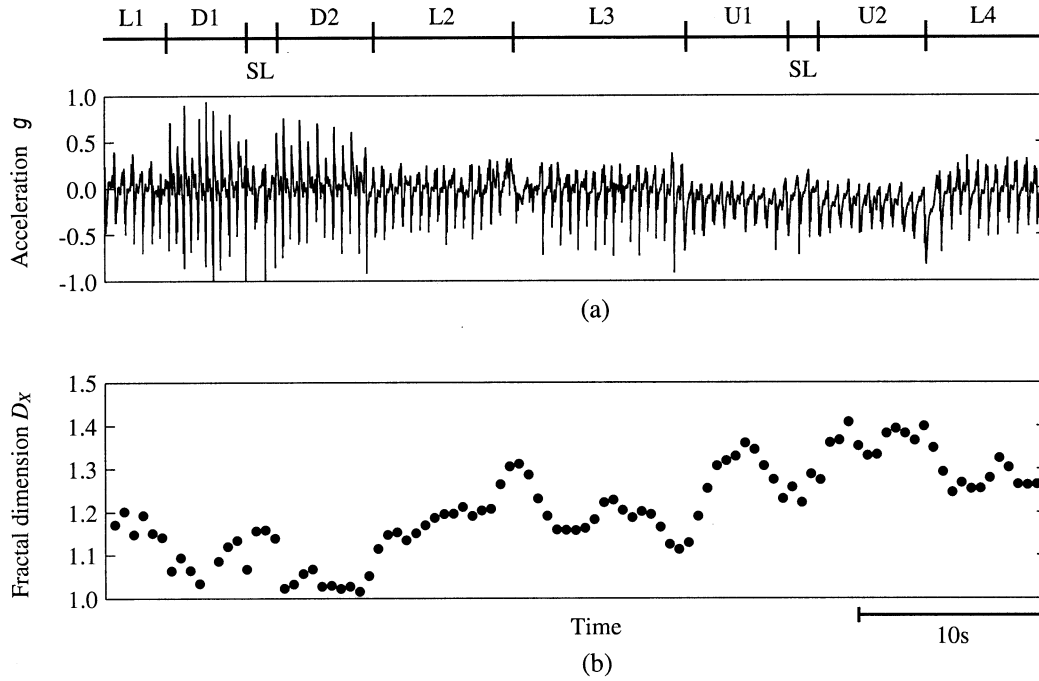
Fig. 5. Typical examples of the acceleration in the x direction and its fractal dimension over time. The segments along the x axis are shown in Fig. 2. The fractal dimension was estimated by using the slope of legalism of variances of d_{2j} on scales 7 to 1.

TABLE I
THE AVERAGE VALUES OF THE FRACTAL DIMENSIONS AT EACH SEGMENT SHOWN IN FIG. 2

Subject	Age	D_X			D_Y			D_Z		
		Level	Down	Up	Level	Down	Up	Level	Down	Up
#1	24	1.107	1.122	1.277	1.097	1.123	1.217	1.170	1.107	1.217
#2	20	1.210	1.230	1.307	1.226	1.237	1.255	1.291	1.238	1.259
#3	24	1.234	1.214	1.328	1.319	1.388	1.319	1.323	1.376	1.256
#4	20	1.223	1.105	1.342	1.138	1.111	1.265	1.122	1.134	1.247
#5	20	1.163	1.110	1.219	1.095	1.120	1.216	1.108	1.169	1.285
#6	25	1.177	1.272	1.274	1.152	1.139	1.235	1.156	1.237	1.268
#7	22	1.200	1.097	1.440	1.263	1.176	1.335	1.194	1.186	1.204
#8	24	1.259	1.243	1.378	1.204	1.133	1.219	1.203	1.248	1.243
#9	24	1.277	1.185	1.344	1.286	1.204	1.274	1.248	1.229	1.213
#10	23	1.273	1.148	1.309	1.452	1.150	1.218	1.294	1.160	1.231
#11	60	1.314	1.347	1.516	1.195	1.348	1.422	1.241	1.358	1.419
#12	71	1.261	1.307	1.493	1.232	1.264	1.382	1.122	1.182	1.248
#13	73	1.396	1.436	1.612	1.369	1.426	1.513	1.304	1.268	1.357
#14	80	1.374	1.265	1.448	1.376	1.362	1.382	1.311	1.311	1.233
#15	62	1.173	1.180	1.420	1.262	1.227	1.352	1.244	1.202	1.209
#16	68	1.174	1.250	1.340	1.085	1.159	1.268	1.143	1.200	1.272
#17	67	1.249	1.378	1.605	1.269	1.306	1.517	1.164	1.299	1.425
#18	64	1.338	1.298	1.431	1.258	1.073	1.282	1.184	1.136	1.246
#19	70	1.204	1.219	1.274	1.177	1.134	1.243	1.177	1.114	1.182
#20	69	1.131	1.231	1.332	1.167	1.211	1.255	1.095	1.119	1.189
#21	73	1.261	1.260	1.473	1.254	1.228	1.381	1.196	1.127	1.262
#22	72	1.269	1.270	1.503	1.233	1.198	1.354	1.234	1.237	1.304

($p < 0.01$). In fractal dimension D_Y, the differences between level and downstairs, level and upstairs, and downstairs and upstairs were statistically significant within 16 of 22, 17 of 22, and 17 of 22 subjects, respectively ($p < 0.01$). In fractal dimension D_Z, the differences between level and downstairs, level and upstairs, and downstairs and upstairs were statistically significant within 15 of 22, 20 of 22, and 18 of 22 subjects, respectively ($p < 0.01$). Therefore, the combination of the fractal dimensions is able to distinguish both walking upstairs and walking downstairs from the other walking types for individual subjects.

We confirmed that the fractal dimensions could be reproduced well, as shown in Fig. 6 and Table II. The correlation coefficients r between the first trial and the second trial were high for all three directions. Moreover, the paired t test revealed that the differences between the first and second trial are not statistically significant.

Fig. 7 shows typical examples of the variance of d_{2j} at scales 7 to 1 in the x direction during level walking. We can see from this figure that the variances of d_{2j} decreased with aging and with Parkinson's disease and that their slopes were less steep.
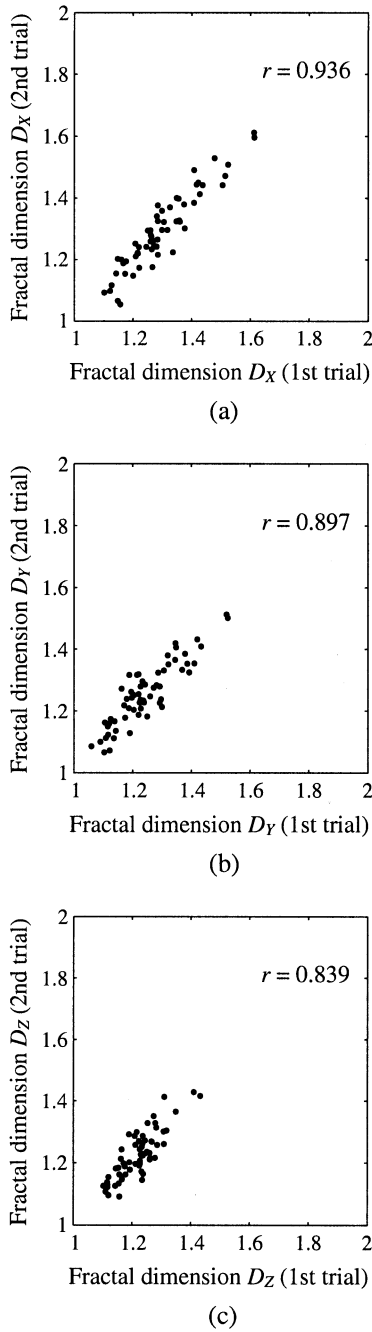
Fig. 6. Reproducibility of the fractal dimensions: 22 subjects, three types of walking.

TABLE II
REPRODUCIBILITY DATA (22 SUBJECTS, THREE TYPES OF WALKING)

	1st trial		2nd trial		Correlation coefficient r
	Mean	SD	Mean	SD	
D_X	1.298	0.117	1.295	0.126	0.936
D_Y	1.243	0.105	1.256	0.103	0.897
D_Z	1.221	0.069	1.228	0.079	0.839

Table III shows the comparisons of fractal dimensions between the healthy young subjects and elderly subjects during level walking. The fractal dimension D_X was shifted from 1.206 ± 0.088 in young subjects to 1.267 ± 0.098 in elderly
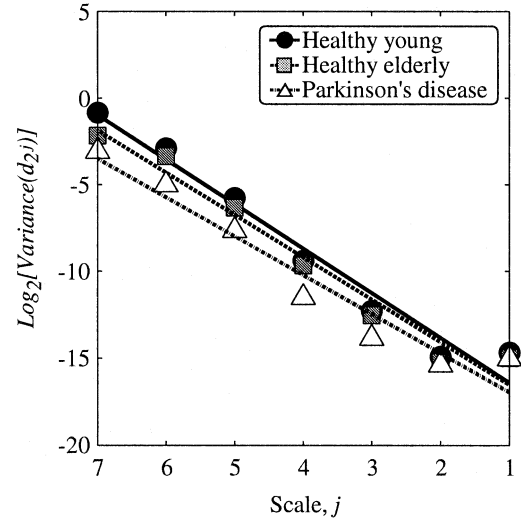

Fig. 7. Typical examples of the variance of d_{2j} on scales 7 to 1 in the x direction during level walking. The circles, squares, and triangles indicate the variance of d_{2j} in a healthy young subject, in a healthy elderly subject, and in a patient with Parkinson's disease, respectively.

TABLE III
COMPARISONS OF FRACTAL DIMENSION BETWEEN THE YOUNG SUBJECTS AND THE ELDERLY SUBJECTS DURING LEVEL WALKING

	D_X^*		D_Y^*		D_Z	
	Mean	SD	Mean	SD	Mean	SD
Young ($n = 10$)	1.206	0.088	1.215	0.131	1.208	0.092
Elderly ($n = 12$)	1.267	0.098	1.249	0.096	1.205	0.085

* : $p < 0.01$, significant difference.

TABLE IV
THE FRACTAL DIMENSIONS IN THE PATIENTS WITH PARKINSON'S DISEASE DURING LEVEL WALKING

Patient	D_X		D_Y		D_Z	
	Mean	SD	Mean	SD	Mean	SD
#1	1.338	0.042	1.242	0.043	1.247	0.042
#2	1.379	0.039	1.485	0.037	1.249	0.034

subjects. The fractal dimension D_Y was also shifted from 1.215 ± 0.131 in young subjects to 1.249 ± 0.096 in elderly subjects. These fractal dimensions were statistically analyzed using the Wilcoxon rank sum test. They were significantly higher for the elderly subjects than for the young subjects ($p < 0.01$). Thus, the fractal dimension appears to increase with aging.

Table IV shows the fractal dimensions in the patients with Parkinson's disease. For these patients, the fractal dimensions tended to be higher. These results suggest that the acceleration signals change into a more complex pattern with aging and with Parkinson's disease.

VI. DISCUSSION

In this paper, we attempted to classify the acceleration signals for walking along a corridor and on stairs by using wavelet-based fractal analysis. In addition, wavelet-based
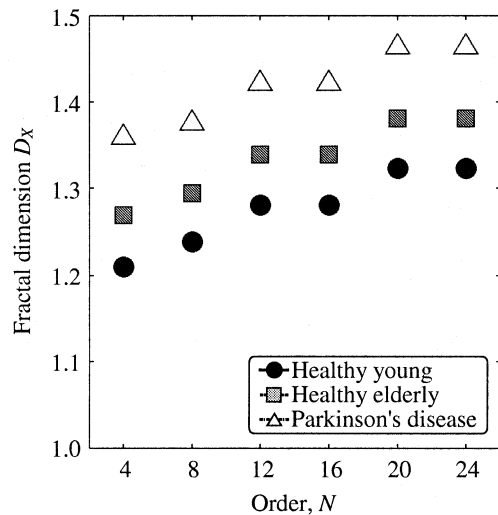
Fig. 8.   Comparison of the fractal dimension D_X calculated by using different order wavelet filters. The circles, squares, and triangles indicate the fractal dimension D_X during level walking in a typical healthy young subject, a typical healthy elderly subject, and a patient with Parkinson's disease, respectively.

fractal analysis was applied to evaluate the gait of elderly subjects and patients with Parkinson's disease. The wavelet-based approach was chosen since it has been found to be a useful tool for analysis of nonstationary biological signals [21], [25], [28]–[31].

This paper demonstrates that the fractal dimensions of acceleration signals can be used to characterize walking types. To estimate the fractal dimensions, we used the detailed signals at scales 7 to 1. The frequency band of these signals is approximately 4–512 Hz. It is generally accepted that the frequency corresponding to the step cycle is approximately 2 Hz, and almost all variance of the signal is in the band below 17 Hz. Therefore, it is reasonable to suppose that the detailed signals at scales 7 and 6 are closely related to the impact acceleration, and the other detailed signals are a fluctuation of either locomotion or noise.

In this paper, we only presented the data obtained using the wavelet filter of order 4 since the use of higher order wavelet filters, including the filter order $8, 12, 16, 20,$ and 24, did not improve the separation of the fractal dimensions of the acceleration signals in the healthy young and elderly subjects during the three different types of walking, as detailed in the results section.

Fig. 8 shows the fractal dimensions of the acceleration signal from a typical healthy young patient, a typical healthy elderly patient, and a patient with Parkinson's disease during level walking. This figure shows that the changes in fractal dimensions between these three subjects were consistent regardless of the wavelet filter orders.

During walking upstairs, the impact acceleration decreased since the maximum difference in elevation between the sole and the floor was shorter than with the other walking types. The knee was flexed at the initial floor contact, which attenuated the impact acceleration at the waist, where the accelerometer unit was attached. The decrease of the impact acceleration caused a relative increase in complexity of the acceleration signal, leading to an increase in the fractal dimensions. On the other hand, the fractal dimensions during walking downstairs shifted to values that were either lower or higher than those for level walking.

From examination of the video recording, there are two types of walking downstairs. In type A, the impact acceleration increased because the distance between the sole and the floor was longer than for other walking types. This is in contrast to walking upstairs. However, the impact acceleration decreased in type B walking downstairs. The main reason for this was that the subjects leaned back slightly while walking carefully, thereby changing their center of gravity. Although there were no common features of the fractal dimensions among subjects for walking downstairs, the fractal dimensions were significantly different among the three walking types for individual subjects and showed a high reproducibility (Table II). Therefore, the fractal dimensions were effective for classifying the walking types.

Fractal dimensions could also be used to assess changes in gait caused by either aging or disease. During level walking, elderly subjects characteristically showed shorter stride length than did young subjects [10], [11]. The short stride length resulted from a decrease in the rotational excursions of the pelvis and lower limbs at the instant of heel-strike. Elderly subjects also showed decreases in their peak knee flexion and peak heel elevation during the early swing phase as well as decreases in toe-to-floor distance at the end of the swing phase. Therefore, impact acceleration at the heel-strike was decreased for elderly subjects. Variances of d_{2^j}, which related to impact acceleration, were also decreased and their changes reflected in the fractal dimensions.

Patients with Parkinson's disease walked slowly with a short stride length, similar to the gait of healthy elderly subjects. The patients also showed an increase in disorders of dynamic equilibrium and walking rhythm. In other words, the acceleration signals of patients had more complex patterns than those of the healthy subjects. Therefore, the fractal dimensions were significantly higher for patients with Parkinson's disease than for healthy subjects.

Hausdorff *et al.* examined the fluctuation of locomotion by using a detrend fluctuation analysis (DFA) [32], [33]. Scaling index α, which is determined by DFA, characterizes the self-similarity property of the signal and has direct relation to the slope β, as $\alpha = (\beta + 1)/2$. The scaling index α of stride interval was lower for elderly subjects than for young subjects. Furthermore, α was lower for patients with Huntington's disease than for healthy subjects.

The results of Hausdorff *et al.* have demonstrated that the fluctuations during walking for elderly subjects and patients with Huntington's disease tended to be more random, and the correlations of one stride with nearby strides were reduced. Although we examined patients with Parkinson's disease, rather than Huntington's disease, the two studies yielded similar results. Elderly subjects and patients with Parkinson's disease shuffle along the corridor. In these cases, it is difficult to detect the timing of heel contact and toe-off. Thus, the stride interval cannot be calculated precisely. However, by analyzing

physical acceleration directly, our method is able to evaluate the fluctuation during walking easily in any case.

REFERENCES

[1] H. J. Montoye, R. Washburn, S. Servais, A. Ertl, J. G. Webster, and F. J. Nagle, "Estimation of energy expenditure by a portable accelerometer," *Med. Sci. Sports Exercise*, vol. 15, pp. 403–407, 1983.

[2] C. V. Bouten, K. R. Westerterp, M. Verduin, and J. D. Janssen, "Assessment of energy expenditure for physical activity using a triaxial accelerometer," *Med. Sci. Sports Exercise*, vol. 26, pp. 1516–1523, 1994.

[3] C. V. Bouten, K. T. Koekkoek, M. Verduin, R. Kodde, and J. D. Janssen, "A triaxial accelerometer and portable data processing unit for the assessment of daily physical activity," *IEEE Trans. Biomed. Eng.*, vol. 44, pp. 136–147, Mar. 1997.

[4] M. Makikawa and H. Iizumi, "Development of an ambulatory physical activity memory device and its application for the categorization of actions in daily life," in *Proc. Medinfo. '95* , 1995, pp. 747–750.

[5] J. Fahrenberg, Foerster, Smeja, and W. Müller, "Assessment of posture and motion by multichannel piezoresistive accelerometer recordings," *Psychophysiology*, vol. 34, pp. 607–612, 1997.

[6] P. H. Veltink, B. J. Bussmann, de Vries, L. J. Martens, and R. C. V. Lummel, "Detection of static and dynamic activities using uniaxial accelerometers," *IEEE Trans. Rehab. Eng.*, vol. 4, pp. 375–385, Dec. 1996.

[7] K. Aminian, R. Jéquier, and Y. Schutz, "Estimation of speed and incline of walking using neural network," *IEEE Trans. Instrum. Meas.* , vol. 44, pp. 743–746, June 1995.

[8] T. Tamura, M. Sekine, M. Ogawa, T. Togawa, and Y. Fukui, "Classification of acceleration waveforms during walking by wavelet transform," *Meth. Inform. Med.*, vol. 36, pp. 356–359, 1997.

[9] M. Sekine, T. Tamura, T. Togawa, and Y. Fukui, "Classification of waist-acceleration signals in a continuous walking record," *Med. Eng. Phys.*, vol. 22, pp. 285–291, 2000.

[10] M. P. Murray, A. B. Drought, and R. C. Kory, "Walking patterns in normal men," *J. Bone Joint Surg.*, vol. 46-A, pp. 335–360, 1964.

[11] M. P. Murray, R. C. Kory, and B. H. Clarkson, "Walking patterns in healthy old men," *Gerontology*, vol. 24, pp. 169–178, 1969.

[12] N. Özgirgin, N. Bölükbaşi, M. Beyazova, and S. Orkun, "Kinematic gait analysis in hemiplegic patients," *Scand. J. Rehab. Med.*, vol. 25, pp. 51–55, 1993.

[13] S. Morita, H. Yamamoto, and K. Furuya, "Gait analysis of hemiplegic patients by measurement of ground reaction force," *Scand. J. Rehab. Med.*, vol. 27, pp. 37–42, 1995.

[14] G. A. Spolek and F. G. Lippert, "An instrumented shoe—A portable force measuring device," *J. Biomech.*, vol. 9, pp. 779–783, 1976.

[15] M. Kljajic and J. Krajnik, "The use of ground reaction measuring shoes in gait evaluation," *Clinical Phys. Physiol. Meas.*, vol. 8, pp. 133–142, 1987.

[16] S. Miyazaki and A. Ishida, "Capacitive transducer for continuous measurement of vertical foot force," *Med. Biol. Eng. Comput.*, vol. 22, pp. 309–316, 1984.

[17] H. S. Zhu, N. Maalej, J. G. Webster, W. J. Tompkins, P. Bach-Y-Rita, and J. J. Wertsch, "An umbilical data-acquisition system for measuring pressures between the foot and shoe," *IEEE Trans. Biomed. Eng.*, vol. 37, pp. 908–911, Sept. 1990.

[18] J. Grampp, J. Willson, and T. Kernozek, "The plantar loading variations to uphill and downhill gradients during treadmill walking," *Foot Ankle International*, vol. 21, pp. 227–231, 2000.

[19] J. R. W. Morris, "Accelerometry—A technique for the measurement of human body movements," *J. Biomech.*, vol. 6, pp. 729–736, 1973.

[20] Y. Brenière and G. Dietrich, "Heel-off perturbation during gait initiation: Biomechanical analysis using triaxial accelerometry and a force plate," *J. Biomech.*, vol. 25, pp. 121–127, 1992.

[21] R. Fischer and M. Akay, "Fractal Analysis of heart rate variability," in *Time Frequency and Wavelets in Biomedical Signal Processing*, M. Akay, Ed.   Piscataway, NJ: IEEE, 1998, pp. 719–728.

[22] B. B. Mandelbrot, *The Fractal Geometry of Nature*. New York: Freeman, 1983.

[23] I. Daubechies, "Orthonormal bases of compactly supported wavelets," *Commun. Pure. Appl. Math.*, pp. 909–996, 1988.

[24] W. G. Wornell and A. V. Oppenheim, "Estimation of fractal signals from noisy measurement using wavelets," *IEEE Trans. Signal Processing*, vol. 40, pp. 611–623, Mar. 1992.

[25] M. Akay and E. J. H. Mulder, "Effects of maternal alcohol intake on fractal properties in human fetal breathing dynamics," *IEEE Trans. Biomed. Eng.*, vol. 45, pp. 1097–1103, Sept. 1998.

[26] P. Flandrin, "On the spectrum of fractional Brownian motions," *IEEE Trans. Inform. Theory* , vol. 35, pp. 197–199, Jan. 1989.

[27] ——, "Wavelet analysis and synthesis of fractional Brownian motion," *IEEE Trans. Inform. Theory* , vol. 38, no. Part 2, pp. 910–917, Mar. 1992.

[28] M. Akay, "Wavelet applications in medicine," *IEEE Spectrum*, pp. 50–56, May 1997.

[29] A. H. Tewfik and M. Kim, "Correlation structure of the discrete wavelet coefficients of fractional Brownian motion," *IEEE Trans. Inform. Theory*, vol. 38, no. Part 2, pp. 904–909, Mar. 1992.

[30] G. W. Wornell, "Wavelet-based representations for the $1/f$ family of fractal processes," *Proc. IEEE* , vol. 81, pp. 1428–1450, Oct. 1993.

[31] P. Flandrin, "On wavelets and fractal processes," in *Time Frequency and Wavelets in Biomedical Signal Processing*, M. Akay, Ed.   Piscataway, NJ: IEEE, 1998, pp. 703–717.

[32] J. M. Hausdorff, P. L. Purdon, C. K. Peng, Z. Ladin, J. Y. Wei, and A. L. Goldberger, "Fractal dynamics of human gait: Stability of long-range correlations in stride interval fluctuations," *J. Appl. Physiol.*, vol. 80, pp. 1448–1457, 1996.

[33] J. M. Hausdorff, S. L. Mitchell, R. Firtion, C. K. Peng, M. E. Cudkowicz, J. Y. Wei, and A. L. Goldberger, "Altered fractal dynamics of gait: Reduced stride-interval correlations with aging and Huntington's disease," *J. Appl. Physiol.*, vol. 82, pp. 262–269, 1997.

Masaki Sekine (S'98–A'01) received the B.S. degree and the M.S. degree in applied electronic engineering and the Ph.D. degree in applied system engineering from Tokyo Denki University, Saitama, Japan, in 1996, 1998, and 2001, respectively. He was a Postdoctoral Fellow at the Department of Gerontechnology at the National Institute for Longevity Sciences, Japan, in 2001.

He is currently a Research Associate at Thayer School of Engineering, Dartmouth College. His current research interests are in biosignal processing, biosignal interpretation, and rehabilitation engineering.

Dr. Sekine is a Member of the Japan Society of Medical Electronics and Biological Engineering. He received the JpCOMPEmbs98 Award of IEEE Japan Chapter of Engineering in Medicine and Biology in 1998 for "classification of acceleration waveform in a continuous walking record."


Toshiyo Tamura (S'75–M'80) received the B.S. and M.S. degrees from Keio University, Japan, in 1971 and 1973, respectively, and the Ph.D. degree from the Tokyo Medical and Dental University in 1980.

He is a Director, Department of Gerontechnology, National Institute for Longevity Sciences, Japan. He also holds several adjunct positions in universities in Japan. His research interests include biomedical instrumentation, biosignal processing, telemedicine, and home care technology.

Dr. Tamura has served as a chair of IEEE/EMBS Tokyo Chapter in 1996–2000 and is the current Asian Pacific representative for the EMBS. He is the Vice Chair of the international committee of the Japanese Society of Medical Electronics and Biological Engineering in 1999–2002.
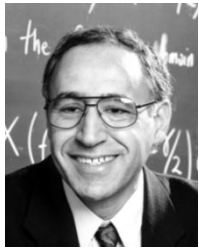
Metin Akay (S'87–M'91–SM'93) received the B.S. and M.S. degrees in electrical engineering from the Bogazici University, Istanbul, Turkey, in 1981 and 1984, respectively, and the Ph.D. degree from Rutgers University, New Brunswick, NJ, in 1990.

He was a Visiting Professor at Rutgers University and is currently an Associate Professor of Engineering, Psychology, and Brain Sciences and Computer Science at Dartmouth College. He has played a key role in promoting biomedical education in the world by writing several prestigious books and editing the first biomedical engineering book series published by Wiley and the IEEE Press and was sponsored by the IEEE EMB Society. The book series had nine published books and eight in press and several pending proposals. He is author/coauthor of 12 books including *Theory and Design of Biomedical Instruments* (New York: Academic, 1991), *Biomedical Signal Processing* (New York: Academic, 1994), *Detection Estimation of Biomedical Signals* (New York: Academic, 1996), *Time-Frequency and Wavelets in Biomedical Engineering* (Wiley and IEEE Press, 1997), *Nonlinear Biomedical Signal Processing* (Wiley and IEEE Press, 2000), *Information Technologies in Medicine* (New York: Wiley, 2000). He is the founding and current editor-in-chief of the first online, interactive Biomedical Engineering and Science Encyclopedia published by Wiley and sponsored with many international organizations. He served as Guest Editor for 12 special issues of the IEEE EMB MAGAZINE, *Annals of BME*, *Journal of BME* in the areas of cardiovascular engineering, virtual reality in medicine, advances in biomedical signal processing, fuzzy logic in medicine. He is also the invited Guest Editor for the PROCEEDINGS OF THE IEEE, the second largest-cited IEEE journal, on neural engineering and for the special issue of the PROCEEDINGS OF THE IEEE on functional genomics, which will be published in 2002. His Neural Engineering and Informatics Lab is interested in investigating the motor functions in patients with Parkinson's disease and post-stroke patients and the effect of developmental abnormalities and maturation on the dynamics of respiration.

Dr. Akay is a member of Eta Kappa, Sigma Xi, Tau Beta Pi, The American Heart Association, and The New York Academy of Science. He also serves on the advisory board of several international journals including the IEEE TRANSACTIONS ON BIOMEDICAL EENGINEERING, IEEE TRANSACTIONS ON INFORMATION TECHNOLOGY IN BIOMEDICINE, and Smart Engineering Systems. He gave several keynote and plenary talks and several invited talks at the international meetings, conferences and symposiums. He is a recipient of the IEEE EMBS Career Service and IEEE Third Millennium Medal. He was the chair of the IEEE EMBS Summer School 1997, 2001, and 2002. He was also the program chair of the Annual IEEE EMBS Conference 2001. He received the IEEE EMBS Early Career Achievement Award (1997) and the Sigma Xi Northeast Young Investigator Award (1998, 2000).

Toshiro Fujimoto received the M.D. degree from the University of Tokyo, Japan, in 1969. He was a Postdoctoral Fellow at the San Pietro Hospital, Paris, France, from 1971 to 1973.

He is currently a chairman at Fujimoto Hayasuzu Hospital, Yoka-kai, Japan. His research interests include magnetic resonance spectroscopy, biomedical measurement, psychiatry and neurology.

Dr. Fujimoto is a Member of Society of Magnetic Resonance Imaging, Japanese Society of Medical Electronics and Biological Engineering, Japanese Society for Magnetic Resonance in Medicine and Japanese Society of Clinical Imaging.

Tatsuo Togawa (M'89–SM'95) received the M.Sc. degree in physics in 1962 and the Ph.D degree in applied physics in 1965 from the University of Tokyo.

Currently, he is a Professor of the Division of Biosystems, Institute of Biomaterials and Bioengineering, Tokyo Medical and Dental University. He has been mainly involved in the research of physiological measurements and instrumentation for more than 35 years.

Dr. Togawa is an Associate Editor of the IEEE TRANSACTIONS ON BIOMEDICAL ENGINEERING. He is a conferred Doctor Honoris Causa, Linkoping University, Sweden (1994) and assigned to Foreign Member, Polish Academy of Science and Member, International Academy of Medical and Biological Engineering (1997).

Yasuhiro Fukui (A'83–M'89) received the B.S. degree in control engineering from the Tokyo Institute of Technology, Tokyo, Japan, in 1967, the M.S. degree in mechanical engineering from Purdue University, West Lafayette, IN, in 1969 and the Ph.D. degree in electrical engineering from the University of Wisconsin, Madison, in 1972, respectively.

He was a Research Fellow with the Department of Anesthesia, University of California, San Diego Medical School from 1972 to 1974. He worked at Fujitsu, Inc., Kanagawa, Japan, in 1974. He joined Tokyo Denki University, Saitama, Japan, in 1977. He is currently a Professor with the Department of Electronic and Computer Engineering, College of Science and Engineering, Tokyo Denki University. He has been the Director of the Frontier Research and Development Center, Tokyo Denki University since 1998. His current research interests are in biomedical control engineering, artificial organs, simulation of biomedical phenomena, and clinical monitoring and welfare engineering.